Challenge Journal of CONCRETE RESEARCH LETTERS

Research Article

Behavior of GGBFS-modified DSM columns in clay soil: Strength–permeability characteristics and predictive laboratory modeling

Murat Olgun [a], Gülsüm Yalçınyiğit [b], Alican Şenkaya [a], Ekrem Burak Toka [a,*], Mustafa Abdalwahid Noori Noori [c], İbrahim Hakkı Erkan [a]

[a] *Department of Civil Engineering, Konya Technical University, 42250 Konya, Türkiye*
[b] *Investments Department of Konya Provincial Health Directorate, 42100 Konya, Türkiye*
[c] *Independent Researcher, 42000 Konya, Türkiye*

ABSTRACT

This study investigated the influence of partially substituting cement with ground granulated blast furnace slag (GGBFS) on the unconfined compressive strength (UCS), splitting tensile strength (STS), and permeability coefficient (k_{DSM}) of deep soil mixing (DSM) columns formed in clay soil. The water/binder ratio was kept constant at 1.0. Cast specimens were prepared using two binder contents, a_w = 15% and 20% by dry soil mass, and five GGBFS substitution ratios of 0%, 10%, 20%, 35%, and 50%. Strength specimens were tested after 7, 28, and 56 days of curing, whereas permeability specimens were tested after 28 and 56 days. Four laboratory-scale DSM columns with a diameter of 300 mm and a length of 600 mm were formed for selected mixtures with a_w = 20% and GGBFS ratios of 0%, 20%, 35%, and 50%; core samples were extracted after 28 days. UCS values ranged from 859 to 4939 kPa, STS from 182 to 830 kPa, and k_{DSM} from 0.16×10^{-10} to 9.17×10^{-10} cm/s for cast specimens. GGBFS reduced early-age strength at 7 days, but improved strength and reduced permeability at later curing ages. The UCS and STS values of core samples were 45.26–69.79% and 63.00–77.58% of the corresponding cast specimen values, respectively, while permeability values of core samples were higher. SEM and XRD observations supported the formation of hydration and pozzolanic products.

ARTICLE INFO

Article history:
Received – April 9, 2026
Revision requested – May 7, 2026
Revision received – May 20, 2026
Accepted – May 26, 2026

Keywords:
Deep soil mixing
Ground granulated blast furnace slag
Permeability
Splitting tensile strength
Unconfined compressive strength

Citation: Olgun M, Yalçınyiğit G, Şenkaya A, Toka EB, Noori MAN, Erkan İH (2026). Behavior of GGBFS-modified DSM columns in clay soil: Strength–permeability characteristics and predictive laboratory modeling. *Challenge Journal of Concrete Research Letters*, 17(2), 207–221.

1. Introduction

Deep soil mixing (DSM) is a ground improvement method that has been widely used in recent years. In this method, in-situ DSM columns are formed by mixing cement and soil. The resulting cement-soil mixture improves the strength and settlement characteristics of soils (Abbey et al. 2015; Chen et al. 2016). The DSM application prevents large shear deformation and excessive settlements, and increases bearing capacity of soils (Shakri et al. 2014). In addition, the water impermeability of the soil is improved.

The production of cement, a building material used in almost all construction processes, results in high amounts of CO_2 emissions, which cause environmental pollution. Roughly one ton of CO_2 is released during the production of one ton of cement (Ganjian et al. 2008; Paniagua et al. 2023). Approximately 8% of the CO_2 released into the atmosphere is related to the cement production process (Ganjian et al. 2015). The use of cement

* *Corresponding author*. E-mail address: ebtoka@ktun.edu.tr (E. B. Toka)
ISSN: 2548-0928 / DOI: https://doi.org/10.20528/cjcrl.2026.02.010

is nevertheless attractive in soil stabilization because it substantially improves soil strength (Holm 2003; Consoli et al. 2015). To reduce cement consumption and its associated environmental impacts, amorphous materials rich in silicates and/or aluminates, such as GGBFS, fly ash (FA), and silica fume (SF), can be incorporated as partial cement substitutes. These industrial by-products can support waste recycling and more sustainable construction practices. Studies on waste-derived binders further show that their contribution is governed by chemical and mineralogical composition, processing conditions, particle characteristics, replacement level, and curing conditions. Consequently, their suitability should be assessed through their combined effects on fresh behavior, mechanical performance, microstructure, and transport properties rather than environmental benefits alone (Mahmud et al. 2025; Mohamad et al. 2025; Ünal and Canbaz 2026; Urbánek and Antoš 2026). Moderate replacement levels may improve particle packing and matrix compactness, whereas excessive substitution may reduce the effective binder content, increase porosity, and adversely affect mechanical or durability-related properties (Turan et al. 2025). Therefore, the partial replacement of cement with suitable industrial by-products represents a potential approach for reducing the environmental impact of soil improvement applications (Lindh and Lemenkova 2022).

GGBFS, a by-product of the steel manufacturing industry, is generally used as a partial cement substitute. This material is mainly composed of calcium oxide (CaO), amorphous silicon dioxide (SiO_2), and aluminum oxide (Al_2O_3). In addition to its pozzolanic properties, GGBFS may exhibit partial hydraulic binding behavior because of the CaO in its chemical composition. Therefore, it can contribute to the development of cementitious bonds when used together with cement. The performance of GGBFS-containing and other fine reactive binder systems is strongly influenced by binder composition, particle fineness, substitution level, water demand, and curing regime, which together govern workability and strength development (Abutaha and Çelik 2025; Shaheen et al. 2025). Considering that slag constitutes approximately 16–20% of steel production by mass (Subathra Devi and Gnanavel 2014) and that less than 50% of the world's waste steel slag is reused (Chaudhary and Pal 2002), the use of GGBFS in DSM column formation offers an important opportunity to reduce cement consumption and promote waste valorization.

Several researchers have investigated the utilization of various industrial waste materials as alternatives to cement for forming DSM columns and soil stabilization (Åhnberg 2006; Abbey et al. 2017; He et al. 2019; Ye et al. 2021; Paniagua et al. 2023; Ramírez and Korkiala-Tanttu 2023; Suksiripattanapong et al. 2023). Some researchers have evaluated in-situ application of DSM (Xue et al. 2024; Forsman et al. 2025; Savila et al. 2025; Swamynaidu and Tyagi 2025). Paniagua et al. (2023) improved a clay soil using bio-ash and slag in combination with cement. Considering the strength and stiffness criteria, they stated that bio-ash and slag can be used as an alternative to cement and lime in soil improvement. Åhnberg (2006) investigated the effect of cell pressure on the strength of a DSM column for specimens prepared using cement, FA and slag; and successfully modeled the DSM column strength for drained and undrained conditions using mathematical equations based on the concept of pre-consolidation pressure and determined the parameters affecting the strength. Suksiripattanapong et al. (2023) investigated the improvement of soft clay soils by DSM with bottom ash and cement. They stated that bottom ash can be used together with cement for both cost reduction and an environmentally friendly DSM column formation process. Ye et al. (2021) investigated the use of binder material containing gypsum and slag as a cement replacement for the improvement of soft soils. The improvement with this binder material resulted in a more rigid structure than cement improvement and a significant increase in strength compared to the unimproved soil. Ramírez and Korkiala-Tanttu (2023) used 6 different low CO_2 emitting binders as an alternative to cement for the improvement of soft clay soils and found that alternative binders for ground improvement not only provide an environmentally friendly solution but also show satisfactory performance in terms of binding properties. He et al. (2019) investigated the effect of the combination of soda residue and GGBFS in soft soils. When these two materials were used together, the strength of the improved soil after 28 days of curing was close to the strength when soda residue and cement were used as binder. Abbey et al. (2017) used pulverized fuel ash and GGBFS with cement for soil stabilization and observed a better improvement in low plasticity soils. They stated that the amount of cement in the binder can be reduced by using GGBFS and pulverized fuel ash. Xue et al. (2024) investigated the application of DSM in soft soils using UCS tests. They observed that UCS values were lower in silty and peat soils than in clay soils and suggested that FA-based cement was suitable for DSM in acidic soils containing organic matter. Savila et al. (2025) evaluated the field applicability of DSM columns. They reported that the strength of field DSM columns met the target values anticipated at the design stage and even increased to more than seven times the target strength after 3.5 years. Swamynaidu and Tyagi (2025) examined the suitability of DSM, which is formed using a certain amount of GGBFS, for in situ use in terms of permeability. They found that permeability decreased significantly with an increase in GGBFS up to 50%, and they developed a correlation between permeability, UCS, and water/binder ratios. Forsman et al. (2025) investigated the usability of 11 different binder types, including GGBFS, in DSM columns, considering lime-cement mixture as a reference. They conducted experiments at six different test sites, focusing on the effects of variables including soil and binder properties on strength changes.

There are limited and insufficient studies simultaneously examining the effects of GGBFS substitution on UCS, STS and k_{DSM} of DSM columns, together with a direct comparison between cast specimens and core samples obtained from laboratory-scale DSM columns. Additionally, there is a lack of research on laboratory-scale model DSM columns that represent in-situ formed DSM columns. The relation between DSM samples prepared as cast specimens in small molds and core samples obtained from laboratory DSM columns is also unclear. In this study, UCS, STS and permeability tests were carried

out on cast specimens to comprehensively investigate the effect of GGBFS on the strength and permeability properties of the DSM columns. Based on the test results on DSM specimens prepared as casting; model DSM columns with a diameter of 300 mm and a length of 600 mm were formed in the laboratory for 4 different designs. The UCS, STS, and k_{DSM} values of core samples extracted from the laboratory DSM columns were compared with those of the cast specimens.

2. Materials and Methods

2.1. Materials and design

The soil used in the study was classified as low plasticity clay (CL) according to the Unified Soil Classification System (USCS) (ASTM D2487 2017). The soil used in this study had a particle size distribution consisting of 8% sand, 34% silt, and 58% clay fraction. The liquid limit of the soil is 33%, the plastic limit is 22%, and the particle density of the soil solids is 2.64 g/cm^3. CEM I 42.5R was used as cement. GGBFS was obtained from Adana Cement Iskenderun Plant and its mineralogical properties are given in Table 1.

The water content of the clay was selected as 27%, which lies between the liquid limit and plastic limit of the soil, to ensure a workable and representative clay consistency. Based on previous studies, binder ratio (a_w; the ratio of the amount of binder to the dry weight of the soil) in DSM applications is generally reported to vary between 10% and 30% (Broms 2003; Bruce et al. 2013; Han 2015; Yu et al. 2021). Within this commonly adopted range, a_w values of 15% and 20% were selected in order to represent moderate and relatively high binder contents that are frequently used in practice, while maintaining workability and avoiding excessive binder consumption. This selection allowed the influence of GGBFS substitution on mechanical and hydraulic properties to be evaluated without introducing extreme binder ratios. Accordingly, GGBFS was used by substituting cement in certain proportions. Previous studies (Åhnberg 2006; Abbey et al. 2017; Paniagua et al. 2023) support the replacement of up to 50% of cement by mass with GGBFS as a reasonable approach. Taking this limit value into account, the ratio of the mass of GGBFS to the total mass of cement+GGBFS was selected as 0, 10, 20, 35 and 50%. These variables and levels were used to establish the design given in Table 2. B, S and D denote a_w, GGBFS and curing period, respectively. The numbers next to the letters represent the percentage for B and S and the number of days for D. For instance, B15S0D7 indicates a mixture with 15% a_w, 0% GGBFS and 7 days curing period. Based on test results, laboratory DSM columns were formed for designs numbered 21, 23, 24 and 25 from Table 2.

Table 1. Chemical composition of the GGBFS.

Chemical composition	SiO_2	Al_2O_3	Fe_2O_3	CaO	MgO	SO_3	K_2O	LOI	Other
Percentage (%)	37.65	13.58	0.92	34.73	8.57	0.95	0.88	0.25	2.47

Table 2. Established design and mixtures.

Design no	Design	a_w (%)	GGBFS (%)	Day	Design no	Design	a_w (%)	GGBFS (%)	Day
1	B15S0D7	15	0	7	16	B20S0D7	20	0	7
2	B15S10D7	15	10	7	17	B20S10D7	20	10	7
3	B15S20D7	15	20	7	18	B20S20D7	20	20	7
4	B15S35D7	15	35	7	19	B20S35D7	20	35	7
5	B15S50D7	15	50	7	20	B20S50D7	20	50	7
6	B15S0D28	15	0	28	21	B20S0D28	20	0	28
7	B15S10D28	15	10	28	22	B20S10D28	20	10	28
8	B15S20D28	15	20	28	23	B20S20D28	20	20	28
9	B15S35D28	15	35	28	24	B20S35D28	20	35	28
10	B15S50D28	15	50	28	25	B20S50D28	20	50	28
11	B15S0D56	15	0	56	26	B20S0D56	20	0	56
12	B15S10D56	15	10	56	27	B20S10D56	20	10	56
13	B15S20D56	15	20	56	28	B20S20D56	20	20	56
14	B15S35D56	15	35	56	29	B20S35D56	20	35	56
15	B15S50D56	15	50	56	30	B20S50D56	20	50	56

2.2. Determining the water/binder ratio

In previous studies (Shen et al. 2012; Takano et al. 2015; Yu et al. 2021), it was suggested that a water/binder ratio of 1.0 was appropriate for the formation of DSM columns. Therefore, a water/binder ratio of 1.0 was selected for both the cast specimens and the laboratory-scale DSM columns. The rheological properties of the grouts were determined using Marsh funnel (ASTM C939 2016) and sedimentation (ASTM C940 2016) tests. The Marsh funnel test (Fig. 1(a)) and sedimentation test (Fig. 1(b)) were used to evaluate the flow times (Fig. 1(c)) and bleeding ratios (Fig. 1(d)) of grouts containing up to 50% GGBFS within the binder. According to the test results, increasing the GGBFS substitution ratio produced a more viscous consistency but did not substantially impair workability or injectability. This rheological response is consistent with observations from blended cementitious systems, in which fine supplementary materials influence flowability by altering specific surface area and water demand, with the magnitude of the effect depending on material reactivity, dosage, and overall mixture composition (Mohamad et al. 2025; Shaheen et al. 2025). S30 and S40, representing 30% and 40% GGBFS substitution, respectively, were used only in the preliminary workability assessment to characterize the continuity of the rheological trends over a wider range of substitution levels and were not included in the main experimental design presented in Table 2.

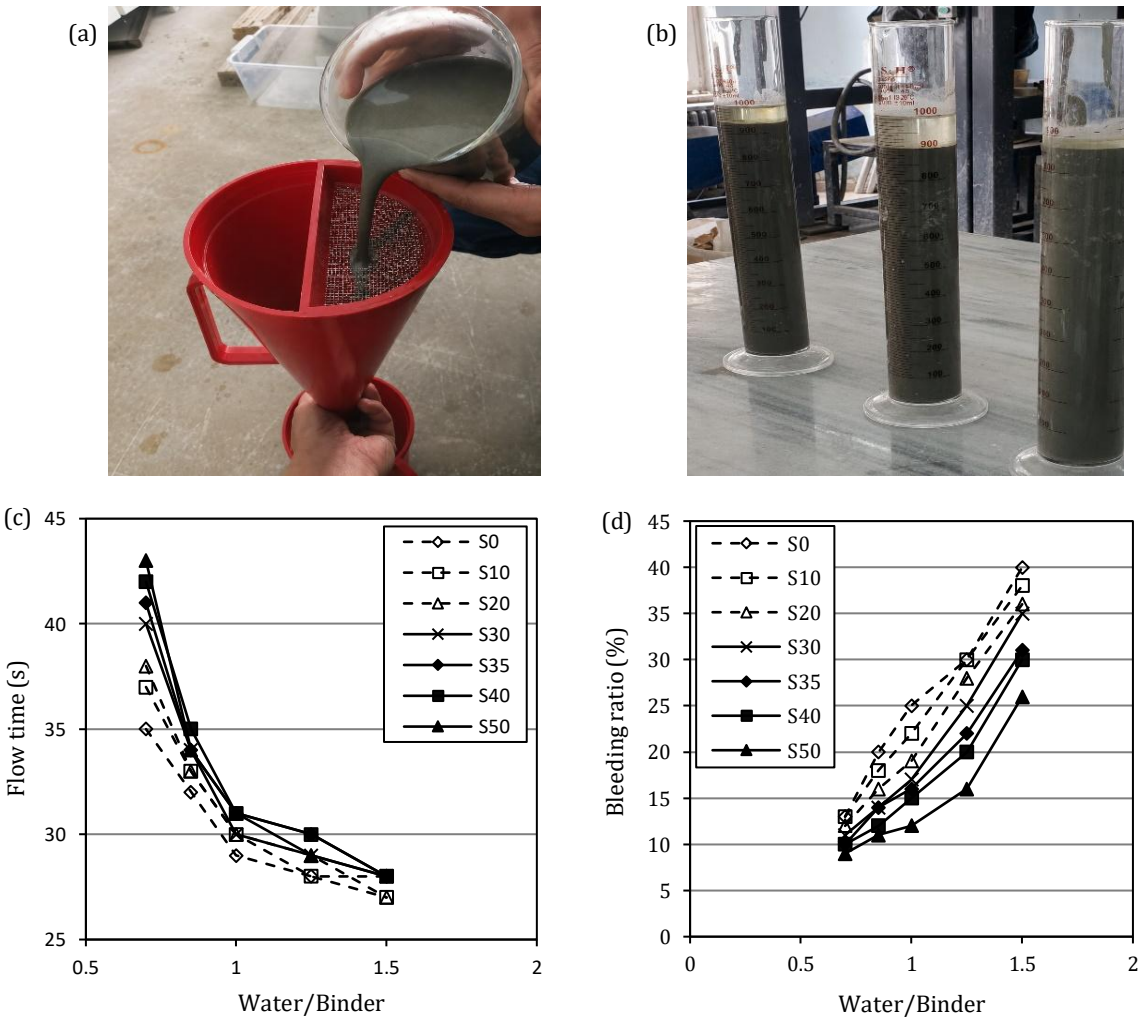

Fig. 1. Preliminary workability studies for mixtures:
(a) Marsh funnel test; (b) Sedimentation test; (c) Flow time; (d) Bleeding ratio.

2.3. Preparation of cast specimens and tests

The clay was dried, ground, and sieved through a 2 mm diameter sieve to prepare cast specimens. The clay, cement, and GGBFS were dry-mixed, and then water was added to achieve both a 27% water content for the clay and a water/binder ratio of 1.0 for the grout. The mixture was mixed for 5 minutes using a laboratory type mixer after adding water to the mixture. Subsequently, the mixture was poured into PVC molds with an inner surface previously coated with grease, having a diameter of 50 mm and a height of 100 mm. Molds with a diameter of 50 mm and a height of 30 mm were used for permeability tests. The mixtures were placed in the molds in three layers. Each layer was properly skewered (Kitazume et al. 2015) to prevent the formation of air pockets within the mixture specimens. To ensure consistency in specimen density, a constant mold volume was used, and the mass of fresh mixture placed into each mold was controlled for each mixture. After demolding,

the specimen dimensions and mass were measured to verify density consistency. In this manner, three samples were prepared for each design, for UCS test (ASTM D4832 2016), STS test (ASTM C496 2017), and permeability test (ASTM D5084 2016). The UCS and STS tests were conducted under displacement control at a rate of 0.5 mm/min. The specimens were cured in air-tight bags at 97±2% relative humidity and 23±2°C for 7, 28, and 56 days. The permeability test specimens were cured for 28 and 56 days. Since curing temperature was kept constant throughout the experimental program, temperature was controlled and was not treated as an independent variable in this study. Permeability tests were performed following ASTM D5084. Each cylindrical specimen was placed within a latex membrane inside the test cell. Saturation was achieved by applying back pressure in incremental steps ensuring full saturation. The cell pressure was maintained at 500 kPa, while back pressure was 450 kPa. A back pressure of 450 kPa was maintained throughout the test and used as the driving hydraulic pressure for water flow through the specimen. The outflow volume measured from a volume change unit connected to the perforated plate beneath the specimen was measured separately, and the k_{DSM} was then calculated using Darcy's law.

2.4. Formation of DSM columns, core sampling and tests

The clay was initially dried, ground, and sieved through a 2 mm diameter sieve to form laboratory DSM columns. Water was added to the clay until 27% water content was achieved and the water and soil were mixed until a homogeneous form was obtained. The mixed soil was placed in a container with a diameter of 600 mm and a height of 900 mm in two stages. The chosen soil water content of 27% is very close to the in-situ water content. The in-situ bulk density (natural/wet density) was previously determined as 1.87 g/cm^3 at 27% water content. Accordingly, the soil was placed in the test container to achieve a density of 1.87 g/cm^3. Since the container volume was known, the container was filled by calculating the mass of soil that could fill this volume. The test container was used only as a laboratory-scale preparation container for forming DSM columns under controlled conditions. No visible or measurable permanent deformation was observed on the HDPE container wall before or after column formation. Nevertheless, the possible influence of container rigidity and scale effects should be considered when interpreting the laboratory-scale DSM column results, and the findings should not be directly generalized to field-scale DSM applications without site-specific trial columns and field verification. The prepared soil was allowed to stabilize for two days. After the waiting period, DSM columns were formed. First, CEM I 42.5R, GGBFS, and water were mixed in a separate container to form the injection grout. While the prepared grout was injected into the soil at a constant pressure of 10 bar, a DSM column with a diameter of 300 mm and a length of 600 mm was formed by mechanically mixing the soil using a mixing blade. The injection pressure of 10 bar was selected as it represents typical laboratory-scale DSM mixing pressures and ensures sufficient grout penetration and homogenization in fine-grained soils (Broms 2003; Takano et al. 2015). During the column formation process, the mixing blade was reciprocated vertically five times within the soil to promote uniform mixing and consistent column formation (Fig. 2(a)). This method ensured the reliable formation of DSM columns. The top of the formed columns was covered with plastic bags, and the columns were left to cure for 28 days. Using this method, a total of four DSM columns were formed with an a_w value of 20% and GGBFS substitution ratios of 0%, 20%, 35%, and 50%. The a_w value of 20% was selected based on the cast specimen results, which indicated that this binder ratio provided higher and more stable mechanical performance. Therefore, this value was considered representative for laboratory-scale DSM columns intended to simulate in-situ applications. After the curing period, core sampling of different parts of the columns was done to evaluate strength and permeability properties (Figs. 2(b-c)). The coring machine operated at 1000 rpm during the core sampling. The core sampling process was performed at least four different locations for each DSM column. The core samples were cut to a diameter of 50 mm and a height of 100 mm for UCS and STS tests and were cut to a diameter of 50 mm and a height of 30 mm for permeability tests. The UCS, STS, and permeability tests of core samples were performed using the same methods as for cast specimens. Separate duplicate DSM columns for each mixture were not formed, but the number of core samples extracted was arranged to ensure that at least three samples could be obtained for UCS, STS and permeability test.

2.5. Statistical analysis using ANOVA

Statistical analysis was performed using analysis of variance (ANOVA) to evaluate the significance of the effects of a_w, GGBFS content, and curing period on UCS, STS, and k_{DSM}. ANOVA was selected as it allows the assessment of both individual factors and their interaction effects on the measured responses. The significance level was set at $p < 0.05$, corresponding to a 95% confidence level, which is commonly adopted in geotechnical and materials engineering studies. Model adequacy was evaluated using the coefficient of determination (R^2).

3. Results and Discussion

3.1. UCS of cast specimens

UCS test results were given in Fig. 3 and stress-strain curves of some selected designs were presented in Fig. 4. For cast specimens, the highest UCS was obtained for B20S50D56 with 4939 kPa and the lowest UCS was obtained for B15S50D7 with 859 kPa (Fig. 3). As the curing period increased, the strength increased as expected. The increase in the GGBFS ratio caused an initial decrease in strength at 7 days curing but significant increase in strength at the end of 28 and 56 days of curing. A similar behavior was observed in a study by Estabragh et al. (2016). Compared with the non-GGBFS reference specimens, the UCS values of the GGBFS-containing specimens corresponded to 73–98% of the reference at 7

days, 105–179% at 28 days, and 110–171% at 56 days as the GGBFS substitution ratio increased from 10% to 50%. The fundamental reason for the increase in strength with the use of GGBFS is due to the pozzolanic properties (Lindh and Lemenkova 2022) of GGBFS reacting with the calcium hydroxide (CH – $Ca(OH)_2$) formed as a result of hydration, thereby creating calcium-silicate-hydrates (C-S-H). Owing to its chemical composition, GGBFS can partially react with clay minerals in a way similar to cement–clay interactions (Richardson et al. 1994; Nidzam and Kinuthia 2010). However, since the hydration reaction capability of GGBFS alone is weak, the use of GGBFS without an additional activating agent like cement would not be appropriate (Yi et al. 2014). Thus, it was observed that cement and GGBFS work effectively together.

Fig. 2. DSM column formation and core sampling:
(a) DSM column formation in preparation container; (b) Core sampling; (c) Core samples.

The reason for the decrease in strength with an increase in the GGBFS ratio when the curing period is 7 days is that a 7-day curing period is not sufficient for the occurrence of pozzolanic reactions; because pozzolanic reactions develop and continue over a longer period (Davidson et al. 1965; Sargent 2015). When examining the model equation given in the ANOVA results (Table 3), the negative coefficient of GGBFS for the 7-day curing period is an indicator of this phenomenon. Accordingly, the positive effect of GGBFS on strength became evident as the curing period increased. The increase in strength was significant when the curing period was extended from 7 to 28 days, whereas the strength gain was comparatively smaller between 28 and 56 days. Therefore, the pozzolanic reactions of GGBFS continued in a time-dependent manner (Nidzam and Kinuthia 2010) and these reactions were more effective from 7 to 28 days in this study. In the ANOVA results (Table 3), the F-value of the interaction term of GGBFS and curing period being 45.20 and the F-value of the GGBFS term being 81.58, indicates that GGBFS was effective on the strength with the length of curing period. An R^2 of 97.84% and a p-value smaller than 0.05 indicate that this model is significant. It can be said that the model equation will be consistent in predicting the strength of the cast specimen, provided that the variables used in this study remain within the lowest and highest-level limits (in the model equations, the unit of a_w and GGBFS are "%" and the unit of UCS is "kPa"). Some terms in the UCS model had p>0.05 and are therefore statistically insignificant at the 95% confidence level; however, they were retained in the fitted equation for model interpretability and should not be interpreted as significant individual effects.

3.2. STS of cast specimens

Although natural clayey soils typically exhibit negligible tensile strength, cement and cement-GGBFS-stabilized DSM columns behave as semi-rigid structural elements that may be subjected to tensile and bending stresses under various loading scenarios. Specifically, tensile strength is critical in the following situations: (i) edge columns within group configurations under eccentric vertical loading, where bending moments induce tensile stresses on the column tension face (Kitazume and Maruyama 2007); (ii) seismic loading conditions, where lateral inertia forces produce bending and tensile failures, particularly in the upper portion of the columns (Boufarh et al. 2025); (iii) lateral spreading and liquefaction-induced kinematic forces in earthquake-prone regions; (iv) excavation-induced asymmetric earth pressures on retaining DSM walls; and (v) embankment loading, where columns near the slope toe experience significant bending moments. Recent comparative analyses

have shown that DSM columns can fail predominantly in tilting and bending modes (Fulambarkar et al. 2025), indicating that shear strength alone is insufficient to characterize their failure behavior. Accordingly, characterizing both UCS and STS provides a more complete description of the mechanical response of GGBFS-modified DSM columns and supports rational design under multidirectional loading scenarios.

For the cast specimens, the highest STS was 830 kPa for the B20S50D56, while the lowest STS was 182 kPa for the B15S50D7 (Fig. 5). The prolongation of the curing period increased STS. Increase in the GGBFS ratio led to an initial decrease in strength at 7 days curing but increase in strength at the end of 28 and 56 days of curing. The reasons behind these results are similar to the increase observed in UCS. For the 7-day curing period, there was a decrease in the STS with the increase in the ratio of GGBFS, while the STS increased with increasing GGBFS ratio at 28 and 56 days of curing. In other words, insufficient curing period combined with the presence of GGBFS in the binder negatively affected the strength. Conversely, as the curing period increased, continued hydration and pozzolanic reactions contributed to an increase in STS. Furthermore, in the established statistical model, the interaction term of GGBFS and curing period had an F-value of 17.2 and the GGBFS term had an F-value of 52.26 (Table 4), indicating that GGBFS significantly influenced strength in conjunction with curing time. Compared with the non-GGBFS reference specimens, the STS values of the GGBFS-containing specimens ranged from 92% to 98% of the reference at 7 days, from 104% to 151% at 28 days, and from 103% to 165% at 56 days as the GGBFS substitution ratio increased from 10% to 50%. The ANOVA results demonstrated that this model is a significant model with an R^2 of 95.97% and a p-value of <0.05, and that the STS for cast specimens can be predicted with high accuracy with this model (in the model equation, the units of a_w and GGBFS are "%" and the unit of STS is "kPa").

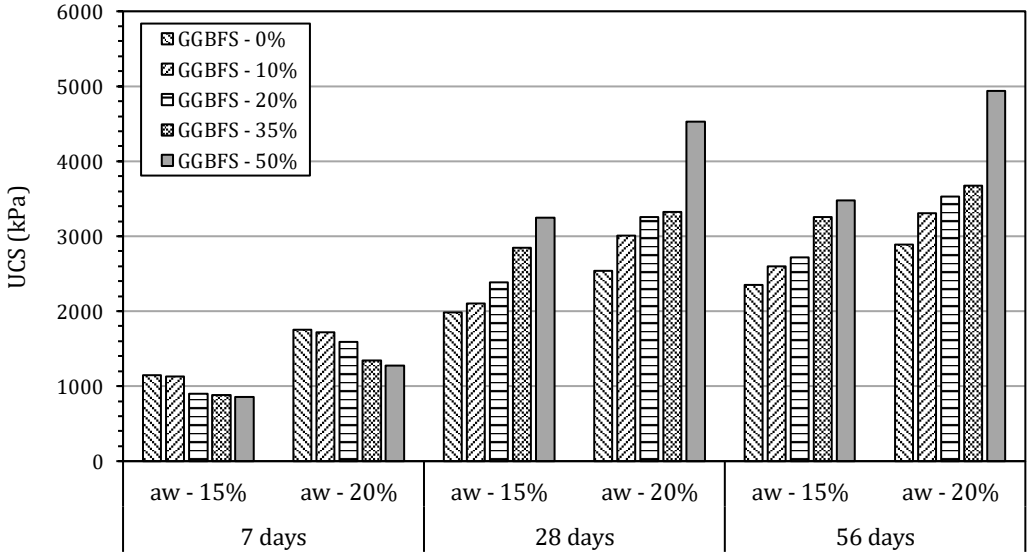

Fig. 3. UCS with respect to curing period, a_w and GGBFS ratio for cast specimens.

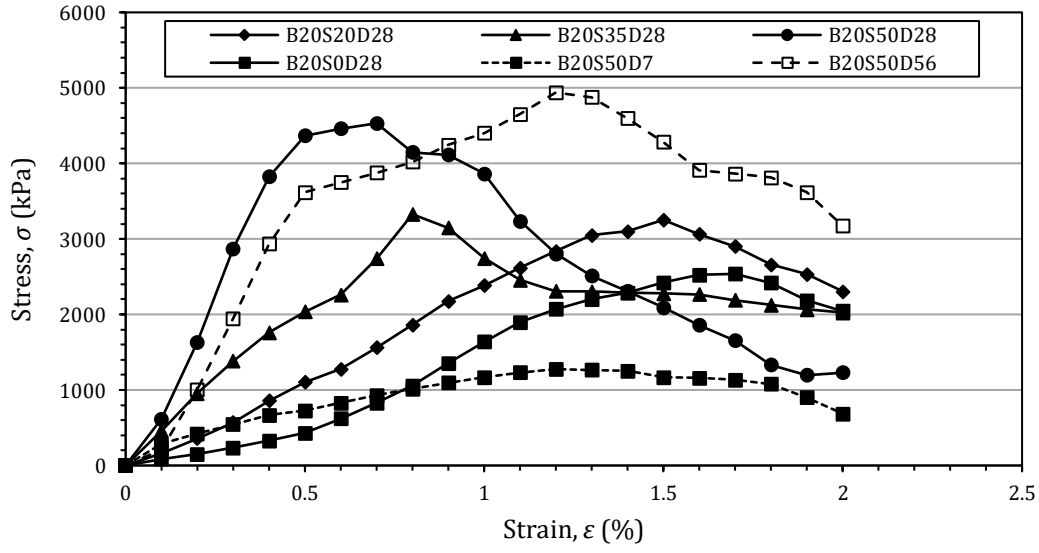

Fig. 4. Stress-strain curves of the selected designs.

Table 3. ANOVA results for UCS.

Source	Degrees of freedom	Sum of squares	Mean square	F-value	P-value
Model	8	33209393	4151174	118.67	<0.001
a_w (%)	1	3880084	3880084	110.92	<0.001
GGBFS (%)	1	2853762	2853762	81.58	<0.001
Day	2	23132028	11566014	330.64	<0.001
GGBFS^2	1	102727	102727	2.94	0.101
a_w (%) × GGBFS (%)	1	78260	78260	2.24	0.150
GGBFS (%) × Day	2	3162529	1581265	45.20	<0.001
Error	21	734586	34980	–	–
Total	29	–	–	–	–
Model equation	for 7 days: UCS = -529+117.4×a_w -40.1×GGBFS+0.228×GGBFS^2+1.149×a_w×GGBFS				
	for 28 days: UCS = 235+117.4×a_w -0.95×GGBFS+0.228×GGBFS^2+1.149×a_w×GGBFS				
	for 56 days: UCS = 602+117.4×a_w -1.7×GGBFS+0.228×GGBFS^2+1.149×a_w ×GGBFS				

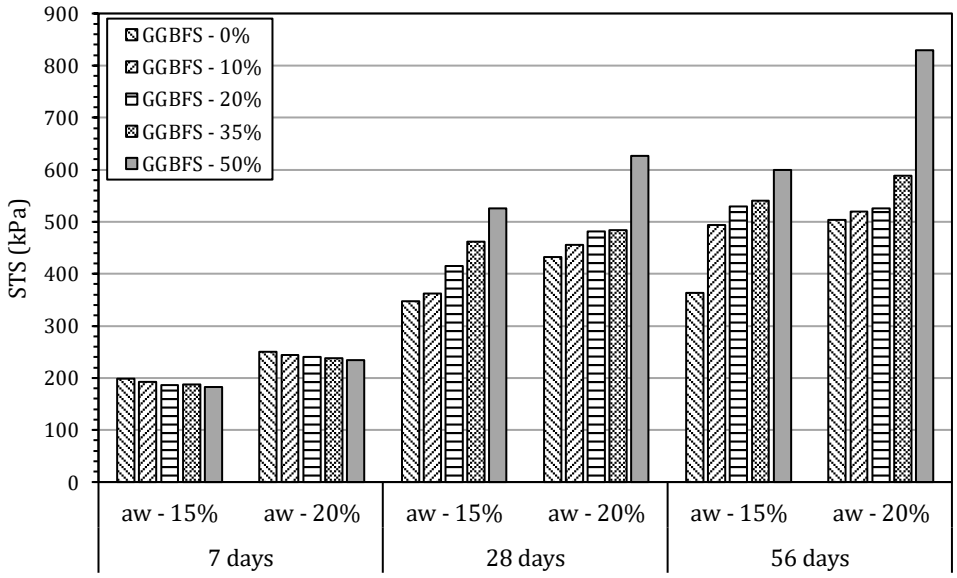

Fig. 5. STS with respect to curing period, a_w and GGBFS ratio for cast specimens.

Table 4. ANOVA results for STS.

Source	Degrees of freedom	Sum of squares	Mean square	F-value	P-value
Model	6	756046	126008	91.22	<0.001
a_w (%)	1	38092	38092	27.58	<0.001
GGBFS (%)	1	72191	72191	52.26	<0.001
Day	2	598200	299100	216.55	<0.001
GGBFS (%) × Day	2	47517	23758	17.20	<0.001
Error	23	31770	1381	–	–
Total	29	–	–	–	–
Model equation	for 7 days: STS = -27.6+14.25×a_w -0.289×GGBFS				
	for 28 days: STS = 128.2+14.25×a_w +3.544×GGBFS				
	for 56 days: STS = 184.6+14.25×a_w +5.024×GGBFS				

3.3. Permeability of cast specimens

The permeability test results indicated that the highest k_{DSM} value of 9.17×10^{-10} cm/s was obtained for B15S0D28, while the lowest k_{DSM} value of 0.16×10^{-10} cm/s was observed for B15S50D56 (Fig. 6). In parallel with the change in UCS and STS, the permeability decreased with the extension of the curing period. In addition, the increase in GGBFS ratio also decreased permeability. The presence of GGBFS, which led to better filling of pores in the specimens (Cheah et al. 2016; Lindh and Lemenkova 2022), was a significant factor in reducing permeability. Therefore, changes in k_{DSM} were influenced not only by UCS and STS but also by hydration and time-dependent pozzolanic reactions. Minor deviations in permeability trends can be attributed to differences in microstructural homogeneity and pore distribution, rather than binder ratio alone, as also supported by the SEM observations presented in Section 3.6. Compared to specimens without GGBFS in the binder, even 10% GGBFS content significantly reduced permeability. Compared with the non-GGBFS reference specimens, the k_{DSM} values of the GGBFS-containing specimens ranged from 18% to 55% of the references at 28 days and from 4% to 38% at 56 days. According to the ANOVA results (Table 5), an R^2 of 92.54% and a p-value of <0.05 indicate that the established model is statistically significant (in the model equations; the unit of GGBFS is "%" and the unit of k_{DSM} is "cm/s", ANOVA was performed for $k_{DSM}\times10^{10}$ cm/s). The ANOVA results showed that k_{DSM} for the cast specimens prepared in the laboratory can be predicted accurately using the model equations (Table 5).

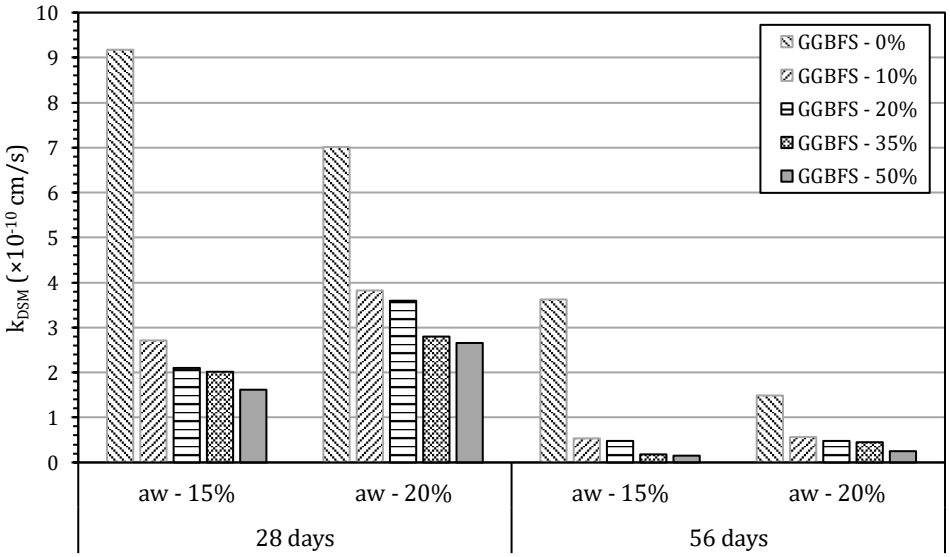

Fig. 6. k_{DSM} values with respect to curing period, a_w and GGBFS ratio for cast specimens.

Table 5. ANOVA results for k_{DSM} values.

Source	Degrees of freedom	Sum of squares	Mean square	F-Value	P-Value
Model	4	25.62	6.40	46.50	<0.001
GGBFS (%)	1	7.04	7.04	51.09	<0.001
Day	1	17.48	17.48	126.87	<0.001
GGBFS²	1	1.16	1.16	8.40	0.011
GGBFS (%) × Day	1	0.650	0.650	4.72	0.046
Error	15	2.07	0.138	–	–
Total	19	–	–	–	–
Model equation	for 28 days: $\ln(k_{DSM}\times10^{10}) = 1.991-0.07\times GGBFS+9.36\times10^{-4}\times GGBFS^2$				
	for 56 days: $\ln(k_{DSM}\times10^{10}) = 0.617-0.09\times GGBFS+9.36\times10^{-4}\times GGBFS^2$				

3.4. Correlation of UCS with STS and k_{DSM}

The relationship between UCS and STS was examined, as shown in Fig. 7(a). The coefficient of determination was R^2 = 94.67%, indicating a strong relationship between UCS and STS. The STS/UCS ratios ranged from 14% to 21%, and the regression equation presented in Fig. 7(a) can be used to estimate STS from UCS within the investigated experimental range. A relationship among UCS, STS, cohesion, and internal friction angle has also been reported for lime-improved soils (Consoli et al. 2014).

The relationship between UCS and k_{DSM} was also examined, as shown in Fig. 7(b). The coefficient of determination was only R^2 = 37.69%, indicating that UCS alone could not reliably predict k_{DSM}. Although mixtures with higher strength generally tended to exhibit lower k_{DSM} values, permeability was also governed by pore connectivity, microstructural homogeneity, and the distribution of hydration and pozzolanic products, as demonstrated by studies on stabilized fine-grained soils and cementitious composites (Lindh and Lemenkova 2022; Cheah et al. 2016). Related research on waste-modified concrete has similarly shown that replacement dosage can simultaneously alter compressive strength and water permeability, with the most favorable balance between these properties occurring at an intermediate replacement level (Mahmud et al. 2025). In the present study, increasing the curing period and GGBFS ratio generally increased UCS and STS while decreasing k_{DSM}. However, the rate of reduction in k_{DSM} did not correspond directly to the rate of increase in UCS. Therefore, a reliable predictive relationship between UCS and k_{DSM} could not be established.

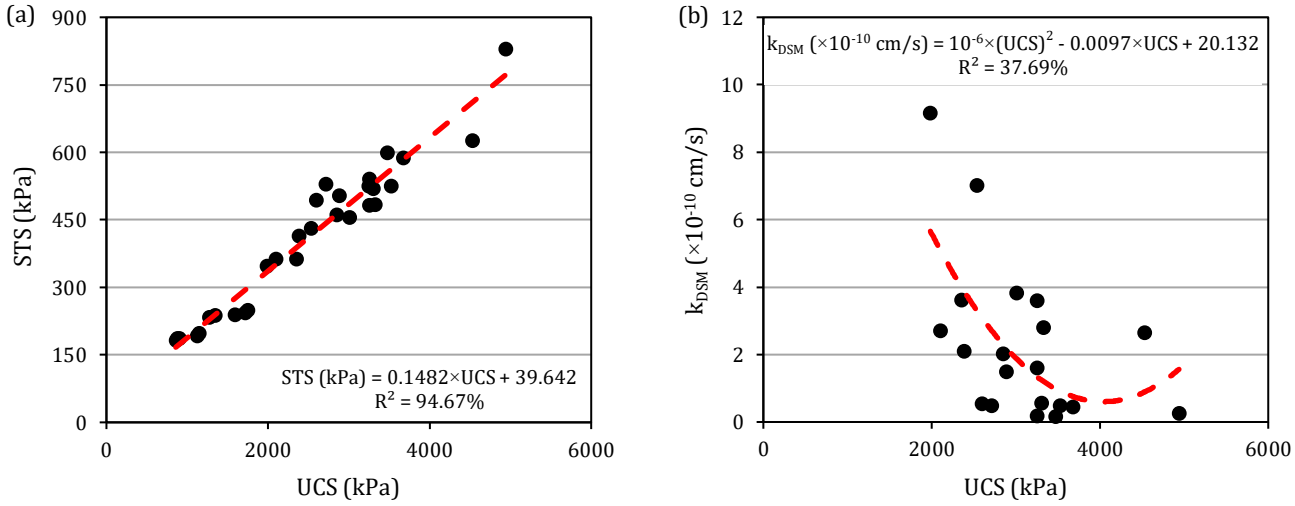

Fig. 7. Correlation between different properties: (a) UCS–STS relationship; (b) UCS–k_{DSM} relationship.

3.5. Comparison of the properties of cast specimens and core samples

The relation between the UCS of the cast specimens and core samples of 4 designs, for which DSM columns were formed, was analysed (Fig. 8(a)). The core sample UCS values were between 45.26% and 69.79% of the cast specimen UCS values. According to the specifications, the core sample strengths of in-situ DSM columns can be 20-50% (EuroSoilStab 2002) and 20-100% (CDIT 2002) or at a minimum 50% (Bruce et al. 2013) of the cast specimen strengths. In this study, since the DSM columns were formed in the laboratory in a similar manner as in-situ application, the ratios of core sample strengths to cast specimen strengths fell within the recommended ranges of specifications. The lower strength of cores from in-situ DSM columns stems from the difficulty of attaining the homogeneity achievable in cast specimens. Therefore, higher strengths are expected for cast specimens. Indeed, in this study, since the core samples extracted from the DSM columns were formed in a manner similar to in-situ applications, their strengths were lower than those of the cast specimens.

A similar result was observed in the comparison between core samples and cast specimens for STS tests (Fig. 8(b)). Accordingly, core sample STS values were 63.00% - 77.58% of the cast specimen STS values. In addition, the comparison of the permeability test results for core samples and cast specimens showed that the core samples were more permeable (Fig. 8(c)). The core sample k_{DSM} values were 118.54% - 193.21% of the cast specimen k_{DSM} values. This relationship reflects the greater microstructural heterogeneity of mixed columns compared with homogeneous cast specimens.

Three mechanisms may contribute to this difference: (i) rotary mixing can produce binder-rich and binder-poor zones within the column matrix, consistent with the cement content variability reported by Zuo et al. (2023) and the in-situ shear strength variability observed by Forsman et al. (2025); (ii) entrapped air voids and partially saturated micro pockets formed during clay–slurry mixing may create preferential flow paths; and (iii) the lower unit weight of model/field DSM columns relative to cast specimens (Saride and Mypati 2024), together with FHWA observations that field-mixed material may attain only 20–50% of laboratory strength, suggests a more open pore structure. Minor coring-induced disturbance cannot be excluded but is considered secondary. From an engineering perspective, this is important for DSM applications where permeability is important such as cut-off walls and containment barriers. In this study, the k_{DSM} of core samples was 1.19–1.93 times higher than that of cast specimens; however, extrapolation to field conditions requires field scale verification. The observed core-to-cast UCS ratios of 45.26% and 69.79% suggest that mechanical performance may be predicted more reliably than hydraulic performance. The results indicated that the strength and permeability of core samples extracted from laboratory DSM columns can be useful in providing a preliminary prediction of the mechanical and hydraulic performance of in-situ DSM columns.

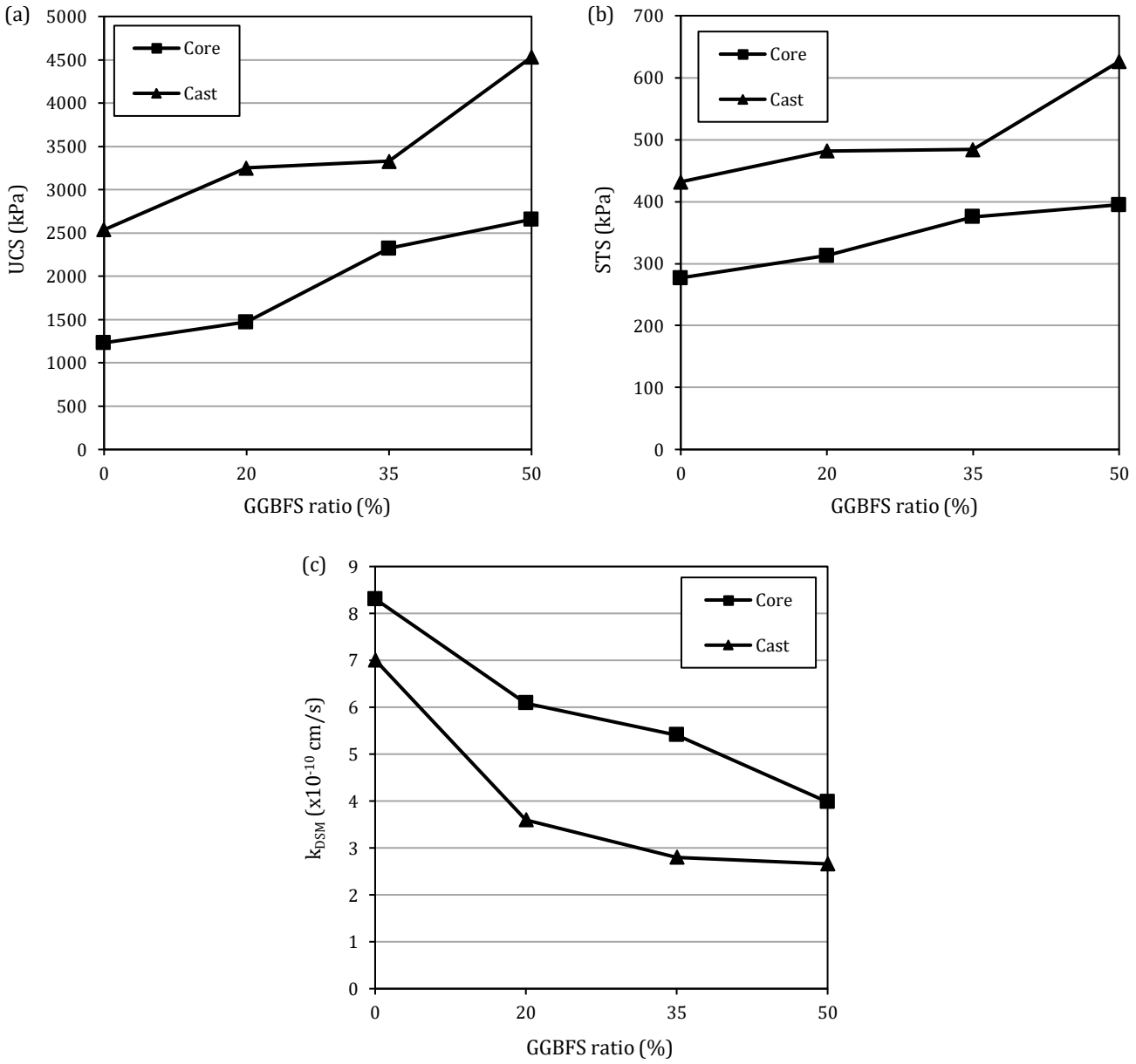

Fig. 8. Comparison of mechanical and hydraulic performance of core samples and cast specimens: (a) UCS values; (b) STS values; (c) k_{DSM} values.

3.6. SEM and XRD analysis results

In the DSM columns, in addition to ettringite, hydration products such as calcium-aluminum-silicate hydrates (C-A-S-H), C-S-H, and CH were identified from SEM images (Fig. 9). As the GGBFS ratio increased, the sample structure became less porous, the amount of C-S-H increased, and C-A-S-H formed. Moreover, the mixture containing 35% GGBFS had a less porous structure than the other samples. As observed from the SEM images, as the GGBFS ratio increased, the amount of C-S-H increased, pores decreased and C-A-S-H formed at 35% GGBFS ratio, which is consistent with the strength and permeability test results of the samples. The increase in UCS and STS and the decrease in permeability as the GGBFS ratio increases are an important indicator of the changing chemical content and amount of pores with the change in the GGBFS ratio on mechanical and hydraulic behavior. Therefore, the strength gain of the samples is primarily attributed to the hydration products formed, namely C-S-H and C-A-S-H, contributing directly to the increase in UCS and STS. The size and amount of pores in the sample structures may also be related to permeability. SEM images also supported the fact that mixtures containing 20% and 35% GGBFS, which had a less porous structure, had lower permeability than the mixture without GGBFS. It was observed that the XRD analysis results (Fig. 10) were consistent with the SEM images. Accordingly, in the presence of cement and GGBFS, peaks were formed in the diffractograms where C-S-H, C-A-S-H, CH and ettringite occurred at the relevant 2θ values. Thus, as determined in the SEM images, it was revealed by the XRD analysis that both hydration and pozzolanic reaction products were formed by mixing the clay soil with cement and GGBFS.

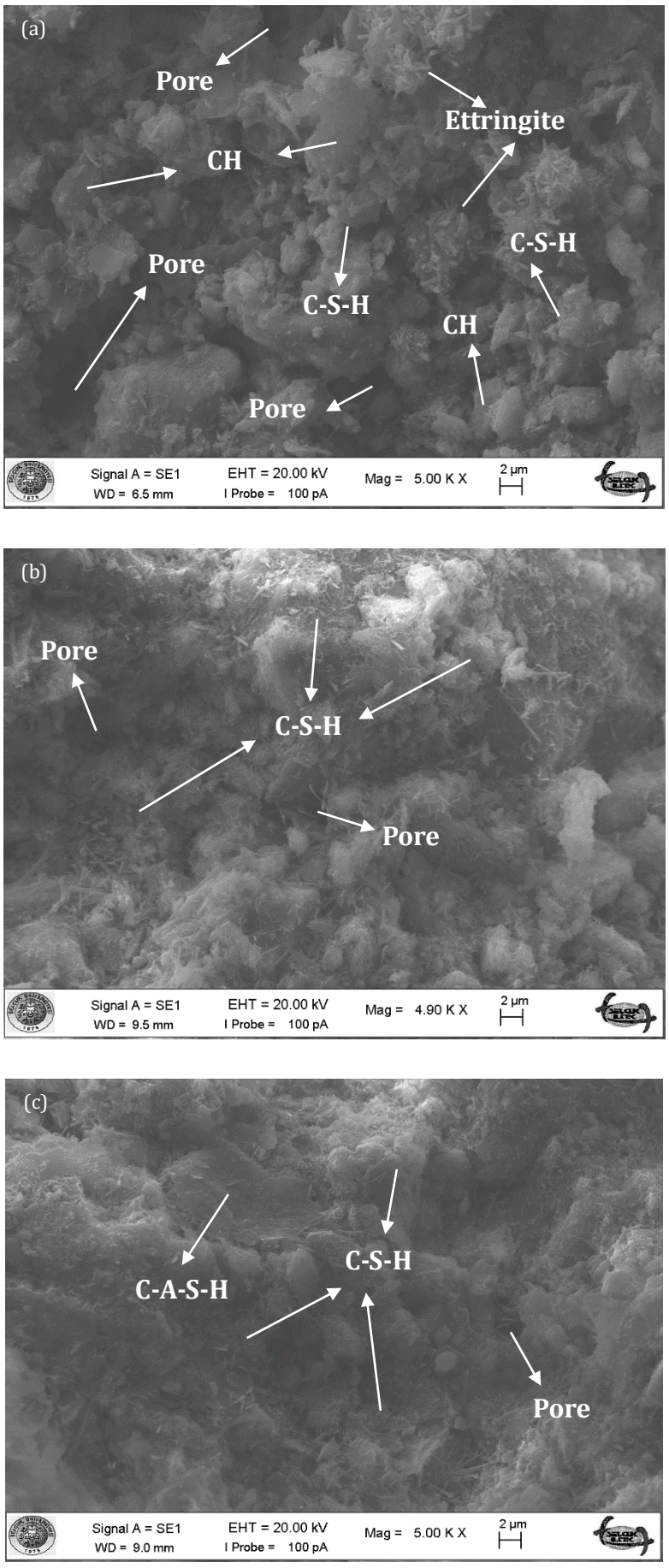

Fig. 9. SEM images for DSM columns: (a) 0% GGBFS; (b) 20% GGBFS; (c) 35% GGBFS.

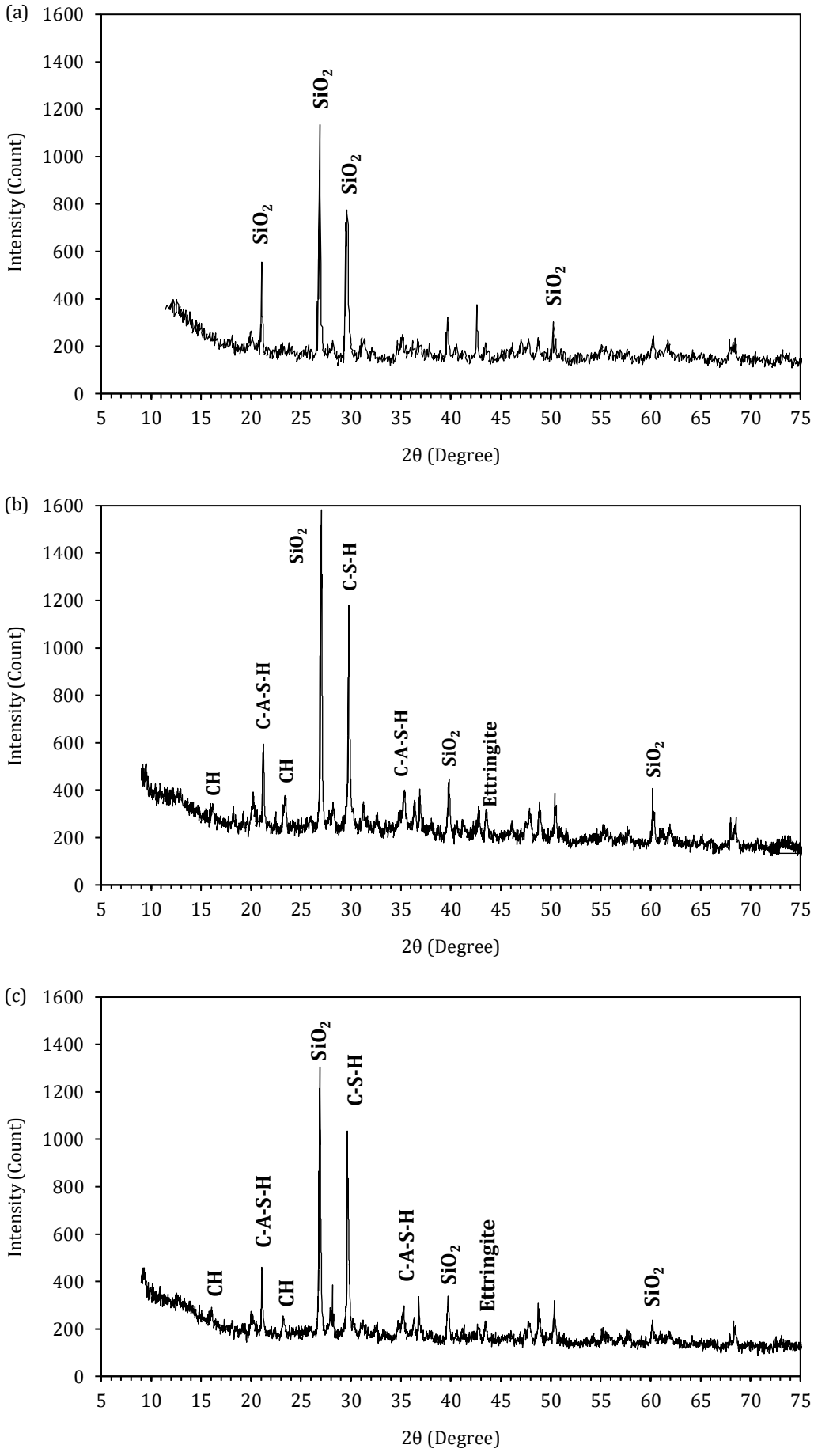

Fig. 10. XRD diffractograms for DSM columns and clay: (a) Clay; (b) 20% GGBFS; (c) 35% GGBFS.

4. Conclusions

In this study, the effect of GGBFS, which is used by substituting cement at certain ratios, on the mechanical and permeability properties of DSM columns was investigated by performing UCS, STS and permeability tests using cast specimens and core samples, and the following results were observed:

- Relative to the corresponding non-GGBFS reference specimens, GGBFS-containing specimens showed lower UCS and STS at 7 days, but higher values at 28 and 56 days, confirming the time-dependent contribution of GGBFS-related hydration and pozzolanic reactions. At 28 and 56 days, UCS reached 105–179% and 110–171% of the reference values, while STS reached 104–151% and 103–165%, respectively.
- The k_{DSM} values of cast specimens decreased with increasing GGBFS substitution. The k_{DSM} values of GGBFS-containing specimens were 18–55% at 28 days and 4–38% at 56 days of the non-GGBFS reference specimens, owing to the pore-filling and additional C-S-H/C-A-S-H formation associated with GGBFS hydration.
- A statistically significant correlation was identified between UCS and STS (R^2 = 94.67%, with STS/UCS = 14–21%), supporting the use of UCS as a reliable predictor of STS within the experimental range. In contrast, the UCS–k_{DSM} relationship yielded R^2 = 37.69%, indicating that permeability is governed by additional microstructural factors that cannot be captured by UCS alone.
- The UCS values of core samples of laboratory-scale DSM columns were 45.26–69.79% of the cast specimen UCS values; STS values were 63.0–77.6%; and k_{DSM} values were 118.5–193.2%. These relationships indicate that laboratory-scale DSM columns may be used as a preliminary tool that laboratory-scale DSM columns can be used as a preliminary tool for evaluating DSM behavior in situ. Laboratory DSM columns exhibited adequate strength and permeability characteristics, demonstrating that effective interactions between soil, cement, and GGBFS can be achieved under controlled laboratory conditions.

Overall, the results suggest that laboratory DSM columns can be effectively used as a preliminary experimental tool to investigate soil–cement–GGBFS interactions and to support the design stage of in-situ DSM applications but not as a direct substitute for field trial columns or site-specific quality control.

Acknowledgements

This publication is based on the master's thesis entitled "Experimental Investigation of Deep Mixing Column Behavior with Blast Furnace Slag Additive".

Funding

This research was supported by Konya Technical University Scientific Research Projects Coordinatorship under grant number 191004004.

Conflict of Interest

The authors declare no potential conflicts of interest with respect to the research, authorship, and/or publication of this manuscript.

Data Availability

The datasets generated and/or analyzed during the current study are not publicly available but are available from the corresponding author upon reasonable request.

AI Assistance

No AI-based tools were used in the preparation of this manuscript.

Author Contributions

All authors made substantial contributions to the conception and design of the study, acquisition of data, analysis and interpretation of data; drafted or critically revised the manuscript for important intellectual content; and approved the final version to be published.

References

Abbey SJ, Ngambi S, Ngekpe BE (2015). Understanding the performance of deep mixed column improved soils: A review. *International Journal of Civil Engineering and Technology*, 6(3), 97-117.

Abbey SJ, Ngambi S, Ganjian E (2017). Development of strength models for prediction of unconfined compressive strength of cement/by-product material improved soils. *Geotechnical Testing Journal*, 40(6), 928-935.

Abutaha F, Çelik Aİ (2025). The engineering properties of silica fume and GGBS-based geopolymer mortars cured in elevated temperature. *Challenge Journal of Concrete Research Letters*, 16(2), 69-84.

Åhnberg H (2006). Consolidation stress effects on the strength of stabilised Swedish soils. *Proceedings of the Institution of Civil Engineers - Ground Improvement*, 10(1), 1-13.

ASTM C496 (2017). Standard test method for splitting tensile strength of cylindrical concrete specimens. ASTM International, West Conshohocken, PA, USA.

ASTM C939 (2016). Standard test method for flow of grout for preplaced-aggregate concrete (flow cone method). ASTM International, West Conshohocken, PA, USA.

ASTM C940 (2016). Standard test method for expansion and bleeding of freshly mixed grouts for preplaced-aggregate concrete in the laboratory. ASTM International, West Conshohocken, PA, USA.

ASTM D2487 (2017). Standard practice for classification of soils for engineering purposes (unified soil classification system). ASTM International, West Conshohocken, PA, USA.

ASTM D4832 (2016). Standard test method for preparation and testing of controlled low strength material (CLSM) test cylinders. ASTM International, West Conshohocken, PA, USA.

ASTM D5084 (2016). Standard test methods for measurement of hydraulic conductivity of saturated porous materials using a flexible wall permeameter. ASTM International, West Conshohocken, PA, USA.

Boufarh R, Aissaoui A, Djellali A, Goudjil K, Boukhatem G, Kırgız MS, Nagaprasad N, Krishnaraj R (2025). Comparative seismic analysis of T-shaped and conventional deep cement mixing columns in highway embankments on soft soil. *Scientific Reports*, 15, 45367.

Broms B (2003). Deep Soil Stabilization: Design and Construction of Lime and Lime/Cement Columns. Royal Institute of Technology, Stockholm, Sweden.

Bruce MEC, Berg RR, Filz GM, Terashi M, Yang DS, Collin JG (2013). Federal Highway Administration Design Manual: Deep Mixing for Embankment and Foundation Support. Technical Report FHWA-HRT-13-046. Federal Highway Administration, Washington, DC, USA.

CDIT (2002). The Deep Mixing Method: Principle, Design and Construction. Coastal Development Institute of Technology, A.A. Balkema Publishers, Lisse, Netherlands.

Chaudhary PN, Pal J (2002). An overview of treatment of steel-making slag for recovery of lime and phosphorus values. *Proceedings of the Seminar on Resurgence of Metallic Materials the Current Scenario (ROMM-2002)*, Jamshedpur, India, 186-190.

Cheah CB, Chung KY, Ramli M, Lim GK (2016). The engineering properties and microstructure development of cement mortar containing

high volume of inter-grinded GGBS and PFA cured at ambient temperature. *Construction and Building Materials*, 122, 683-693.

Chen EJ, Liu Y, Lee FH (2016). A statistical model for the unconfined compressive strength of deep-mixed columns. *Géotechnique*, 66(5), 351-365.

Consoli NC, da Silva Lopes L Jr, Consoli BS, Festugato L (2014). Mohr-Coulomb failure envelopes of lime-treated soils. *Géotechnique*, 64(2), 165-170.

Consoli NC, Winter D, Rilho AS, Festugato L, Teixeira BS (2015). A testing procedure for predicting strength in artificially cemented soft soils. *Engineering Geology*, 195, 327-334.

Davidson LK, Demirel T, Handy RL (1965). Soil pulverization and lime migration in soil-lime stabilization. *Highway Research Record*, 92, 103-126.

Estabragh AR, Khatibi M, Javadi AA (2016). Effect of cement on treatment of a clay soil contaminated with glycerol. *Journal of Materials in Civil Engineering*, 28(4), 04015157.

EuroSoilStab (2002). Development of Design and Construction Methods to Stabilize Soft Organic Soils: Design Guide Soft Soil Stabilization. European Commission, Industrial and Materials Technologies Programme (Brite-EuRam III), Brussels, Belgium.

Forsman J, Löfman M, Ikävalko J, Korkiala-Tanttu L (2025). Low-carbon binders in six test deep mixing cases: Variation of in-situ strength. *Transportation Geotechnics*, 53, 101597.

Fulambarkar S, Manna B, Shahu JT (2025). Effect of deep mixed column pattern on the performance of basal reinforced embankment resting on soft soil. *Soils and Foundations*, 65(2), 101578.

Ganjian E, Sadeghi-Pouya H, Claisse P, Waddell M, Hemmings S, Johansson S (2008). Plasterboard and gypsum waste in a novel cementitious binder for road construction. *Concrete*, 42(6), 20-22.

Ganjian E, Jalull G, Sadeghi-Pouya H (2015). Using waste materials and by-products to produce concrete paving blocks. *Construction and Building Materials*, 77, 270-275.

Han J (2015). Principles and Practice of Ground Improvement. John Wiley & Sons, Hoboken, NJ, USA.

He J, Wang X, Su Y, Li Z, Shi X (2019). Shear strength of stabilized clay treated with soda residue and ground granulated blast furnace slag. *Journal of Materials in Civil Engineering*, 31(3), 06018029.

Holm G (2003). State of practice in dry deep mixing methods. *Proceedings of the 3rd International Conference on Grouting and Ground Treatment*, New Orleans, LA, USA, 145-163.

Kitazume M, Maruyama K (2007). Internal stability of group column type deep mixing improved ground under embankment loading. *Soils and Foundations*, 47(3), 437-455.

Kitazume M, Grisolia M, Leder E, Marzano IP, Correia AAS, Oliveira PJV, Åhnberg H, Andersson M (2015). Applicability of molding procedures in laboratory mix tests for quality control and assurance of the deep mixing method. *Soils and Foundations*, 55(4), 761-777.

Lindh P, Lemenkova P (2022). Permeability, compressive strength and Proctor parameters of silts stabilised by Portland cement and ground granulated blast furnace slag (GGBFS). *Archive of Mechanical Engineering*, 69(4), 667-692.

Mahmud H, Ahmed T, Islam MS (2025). Combined effect of rice husk ash and animal bone powder on strength and permeability of concrete. *Challenge Journal of Structural Mechanics*, 11(1), 1-13.

Mohamad N, Embong R, Othman NH, Muthusamy K, Jaafar MFM (2025). Flowability and compressive strength of ternary blended cement mortar of coal bottom ash and ground cockle shell ash. *Challenge Journal of Concrete Research Letters*, 16(1), 25-32.

Nidzam RM, Kinuthia JM (2010). Sustainable soil stabilisation with blast furnace slag: A review. *Proceedings of the Institution of Civil Engineers - Construction Materials*, 163(3), 157-165.

Paniagua P, Ritter S, Moseid M, Okkenhaug G (2023). Bioashes and steel slag as alternative binders in ground improvement of quick clays. *Proceedings of Geo-Congress 2023: Soil Improvement, Geoenvironmental, and Sustainability*, Los Angeles, CA, USA, 25-34.

Ramírez AL, Korkiala-Tanttu L (2023). Stabilisation of Malmi soft clay with traditional and low-CO2 binders. *Transportation Geotechnics*, 38, 100920.

Richardson IG, Brough AR, Groves GW, Dobson CM (1994). The characterization of hardened alkali-activated blast-furnace slag pastes and the nature of the calcium silicate hydrate (C-S-H) phase. *Cement and Concrete Research*, 24(5), 813-829.

Sargent P (2015). The development of alkali-activated mixtures for soil stabilisation. In: Pacheco-Torgal F, Labrincha JA, Leonelli C, Palomo A, Chindaprasirt P, editors. *Handbook of Alkali-Activated Cements, Mortars and Concretes*. Woodhead Publishing, Sawston, Cambridge, UK, 555-604.

Saride S, Mypati VNK (2024). Effect of area improvement ratio of geopolymer-based deep mixing columns on swell-shrink behavior of expansive soils. *Construction and Building Materials*, 417, 135163.

Savila I-M, Korkiala-Tanttu L, Forsman J, Löfman M (2025). Mechanical properties of stabilized soil: Study on recovered field samples from deep stabilization sites. *Transportation Geotechnics*, 51, 101540.

Shaheen YBI, Etman ZA, Sabiha HL (2025). Design of reactive powder concrete mortar mixes through high strength and durability. *Challenge Journal of Concrete Research Letters*, 16(3), 142-154.

Shakri MS, Hafez MA, Adnan MA, Nazaruddin AT (2014). Effects of use of PFA on strength of stone column and sand column. *Electronic Journal of Geotechnical Engineering*, 19, 3745-3755.

Shen S-L, Xu Y-S, Han J, Zhang J-M (2012). A ten-year review on the development of soil mixing technologies in China. *Proceedings of the 4th International Conference on Grouting and Deep Mixing*, New Orleans, LA, USA, 343-356.

Subathra Devi V, Gnanavel BK (2014). Properties of concrete manufactured using steel slag. *Procedia Engineering*, 97, 95-104.

Suksiripattanapong C, Tesanasin T, Tiyasangthong S, Tabyang W, Sukontasukkul P, Chindaprasirt P (2023). Use of cement and bottom ash in deep mixing application for stabilization of soft Bangkok clay. *Arabian Journal for Science and Engineering*, 48(4), 4583-4593.

Swamynaidu M, Tyagi A (2025). Hydraulic conductivity characteristics of slag-cement clay mixes applicable to in-situ soil mixing techniques. *International Journal of Geosynthetics and Ground Engineering*, 11, 40.

Takano M, Suzuki K, Shinkawa N (2015). Cement deep mixing in Lach Huyen port infrastructure construction project in northern Vietnam. *Proceedings of the Deep Mixing 2015 Conference*, San Francisco, CA, USA.

Turan E, Alameri IA, Oltulu M (2025). Long-term durability of red mud-modified cement mortars: Effects of high temperature and freeze-thaw cycles. *Challenge Journal of Structural Mechanics*, 11(3), 116-127.

Urbánek J, Antoš P (2026). Utilization of fly dust generated during fired shale production for the preparation of aggregates and geopolymers. *Challenge Journal of Concrete Research Letters*, 17(1), 71-81.

Ünal S, Canbaz M (2026). Development of a sustainable geopolymer structural element with waste glass powder: Mechanical characteristics. *Challenge Journal of Structural Mechanics*, 12(1), 22-29.

Xue Z, Zhang W, Zhao X, Meng F, Qin F, Xiao G, Nie Z, Chen J (2024). Utilization of cement deep mixing pile for soft soil foundation: A Malaysian case study. *Frontiers in Materials*, 11, 1484228.

Ye G, Shu H, Zhang Z, Kang S, Zhang S, Wang Q (2021). Solidification and field assessment of soft soil stabilized by a waste-based binder using deep mixing method. *Bulletin of Engineering Geology and the Environment*, 80(6), 5061-5074.

Yi Y, Liska M, Al-Tabbaa A (2014). Properties and microstructure of GGBS-magnesia pastes. *Advances in Cement Research*, 26(2), 114-122.

Yu H, Yi Y, Yao K, Romagnoli A, Tan WL, Chang ABP (2021). Effect of water/cement ratio on properties of cement-stabilized Singapore soft marine clay for wet deep mixing application. *International Journal of Geotechnical Engineering*, 15(9), 1198-1205.

Zuo J, Wang B, Li W, Han S, Wang J, Zhang F (2023). Quality assessment and quality control of deep soil mixing columns based on a cement-content controlled method. *Scientific Reports*, 13, 4813.